[7] Texter et al. examined hydrogen bonding in the crystal structures of 42 proteins solved at high resolution provided eight examples where there are strongly basic residues (Lys, Arg, His) within 4 Å of a proline nitrogen atom that could result in hydrogen bonding to amide nitrogen atoms; see: F. L. Texter, D. B. Spencer, R. Rosenstein, C. R. Matthews, *Biochemistry* **1992**, *31*, 5687 – 5691.

[8] Related 1,8-disubstituted naphthalenes have been reported by Kirby to undergo intramolecular proton transfer catalysis in acetal and enol ether hydrolysis; see: A. J. Kirby, *Acc. Chem. Res.* **1997**, *30*, 290 – 296.

[9] a) F. Hibbert, J. Emsley, *Adv. Phys. Org. Chem.* **1990**, *26*, 255 – 379; b) R. W. Alder, *Chem. Rev.* **1989**, *89*, 1215 – 1223; c) H. A. Staab, T. Saupe, *Angew. Chem.* **1988**, *100*, 895 – 909; *Angew. Chem. Int. Ed. Engl.* **1988**, *27*, 865 – 879. For the orignal report describing the exceptional properties of **2**, see: d) R. W. Alder, P. S. Bowman, W. R. S. Steele, D. R. Winterman, *J. Chem. Soc. Chem. Commun.* **1968**, 723 – 724.

[10] See the Supporting Information for details.

[11] The magnitude of the downfield shift of a hydrogen-bound proton is related to the strength of the bond; see: J. Emsley, *J. Chem. Soc. Rev.* **1980**, *9*, 91 – 125. No coupling was observed in **1a-H**$^+$ between the N-H proton and the methyl protons of the dimethylamino group, as is often noted for the protonated proton sponge **2**.[9]

[12] The observation that the resonances for the *cis* and *trans* isomers coalesce to one upon protonation is consistent with previous reports that predict a lower barrier to rotation about the C – N bond when an amide is N-coordinated to a Lewis acid. See, for example: a) C. Cox, T. Lectka, *J. Am. Chem. Soc.* **1998**, *120*, 10660 – 10668; b) C. Cox, V. G. Young, Jr., T. Lectka, *J. Am. Chem. Soc.* **1997**, *119*, 2307 – 2308; c) C. Cox, D. Ferraris, N. N. Murthy, T. Lectka, *J. Am. Chem. Soc.* **1996**, *118*, 5332 – 5333.

[13] a) G. A. Olah, A. M. White, D. H. O'Brien, *Chem. Rev.* **1970**, *70*, 561 – 591. b) The amide I band is primarily a C=O stretch, and a relationship between C=O bond length and $\nu_{C=O}$ has been found; see A. J. Bennet, V. Somayaji, R. S. Brown, B. D. Santarsiero, *J. Am. Chem. Soc.* **1991**, *113*, 7563 – 7571.

[14] a) The unit cell consists of two molecules of **1b-H**$^+$, two triflate counterions, and one molecule of water. X-ray crystal data for compound **1b-H**$^+$, grown by slow diffusion of Et_2O into a solution of **1b-H**$^+$ in acetone: $C_{21}H_{21}F_4N_2O_{4.50}S$, $M_r = 481.46$, yellow block ($0.30 \times 0.26 \times 0.21$ mm), triclinic, $P\bar{1}$, $a = 12.5179(2)$, $b = 12.9868(1)$, $c = 14.3698(2)$ Å, $\alpha = 87.722(1)$, $\beta = 66.638(1)$, $\gamma = 89.306(1)^\circ$, $V = 2142.84(5)$ Å^3, $Z = 4$, $\rho_{calcd} = 1.492$ Mg m^{-3}, $F(000) = 996$, Siemens SMART Platform CCD, $Mo_{K\alpha}$ radiation, $\lambda = 0.71073$ Å, $T = 173(2)$ K, 10567 reflections collected, 7152 independent reflections, structure solved by direct methods, difference Fourier synthesis, and full-matrix least-squares on F^2 (SHELXTL-V5.0). $R1 = 0.0704$, $wR2 = 0.1688$ for 4744 reflections; the hydrogen atoms on N1A and N1B were located in the Fourier difference map and refined isotropically, all other hydrogens were placed in ideal positions and refined as riding atoms; one of the triflate anions has significant disorder caused by a rocking motion. b) Crystallographic data (excluding structure factors) for the structures reported in this paper have been deposited with the Cambridge Crystallographic Data Center as supplementary publication no. CCDC-104129 (**1b-H**$^+$) and CCDC-104130 (**1b**). Copies of the data can be obtained free of charge on application to CCDC, 12 Union Road, Cambridge CB21EZ, UK (fax: (+44) 1223-336-033; e-mail: deposit@ccdc.cam.ac.uk).

[15] Jeffrey's definition of a "moderately strong hydrogen bond" is inclusive of most biologically relevant interactions, such as the more common hydrogen bonding mode available to amides wherein the oxygen atom is the acceptor; see: G. A. Jeffrey, *An Introduction to Hydrogen Bonding*, Oxford, New York, **1997**, chap. 2.

[16] X-ray crystal data for compound **1b**, grown by slow evaporation of Et_2O: $C_{20}H_{19}FN_2O$, $M_r = 322.37$, colorless block ($0.33 \times 0.24 \times 0.20$ mm), monoclinic, $P2_1/c$, $a = 8.1527(2)$, $b = 10.2495(3)$, $c = 19.5690(6)$ Å, $\beta = 90.305(1)^\circ$, $V = 1635.18(8)$ Å^3, $Z = 4$, $\rho_{calcd} = 1.309$ Mg m^{-3}, $F(000) = 680$, Siemens SMART Platform CCD, $Mo_{K\alpha}$ radiation, $\lambda = 0.71073$ Å, $T = 173(2)$ K, 7755 reflections collected, 2819 independent reflections, structure solved by direct methods, difference Fourier synthesis, and full-matrix least-squares on F^2 (SHELXTL-V5.0). $R1 = 0.0554$, $wR2 = 0.1196$ for 2063 reflections; all hydrogen atoms were placed in ideal positions and refined as riding atoms; disorder was found in the position of the fluorine atom.[14b]

[17] T. Ohwada, T. Achiwa, I. Okamoto, K. Shudo, K. Yamaguchi, *Tetrahedron Lett.* **1998**, 865 – 868.

[18] No transesterification products attributable to ring-opened THF were detected.

[19] a) J. W. Keillor, A. A. Neverov, R. S. Brown, *J. Am. Chem. Soc.* **1994**, *116*, 4669 – 4673; b) J. W. Keillor, R. S. Brown, *J. Am. Chem. Soc.* **1992**, *114*, 7983 – 7989; c) J. W. Keillor, R. S. Brown, *J. Am. Chem. Soc.* **1991**, *113*, 5114 – 5116.

[20] H.-H. Otto, T. Schirmeister, *Chem. Rev.* **1997**, *97*, 133 – 171.

[21] We have recently demonstrated that sponge **1b-H**$^+$ undergoes dramatic intramolecular catalysis of amide isomerization in aqueous solution: C. Cox, H. Wack, T. Lectka, unpublished results.

A Novel Phenylene Topology: Total Syntheses of Zigzag [4]- and [5]Phenylene**

Christian Eickmeier, Daniel Holmes, Heiko Junga, Adam J. Matzger, Frank Scherhag, Moonsub Shim, and K. Peter C. Vollhardt*

Missing from the phenylene topologies hitherto synthesized—linear, angular, and trigonal[1]—is the zigzag variant, exemplified by the title compounds **1a** and **2a**. These

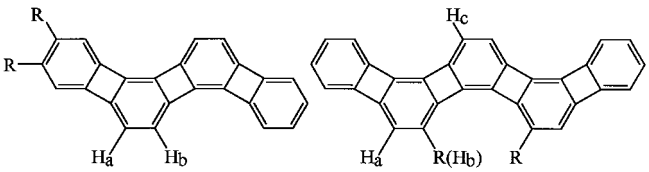

1a, R = H
1b, R = $SiMe_3$

2a, R = H
2b, R = Ph
2c, R = Pr

molecules are important as substructure models for the one-dimensional, zigzag phenylene polymer,[2] the two-dimensional all-carbon net based on the anti-kekulene motif,[1c, 2a, 3] and the three-dimensional carbon allotropes O_h-C_{48}[4] and I_h-C_{120} (archimedene).[5] They are also interesting as members of a family of phenylene isomers with different topologies, in particular in comparison to their angular relatives in which

[*] Prof. Dr. K. P. C. Vollhardt, Dr. C. Eickmeier, D. Holmes, Dr. H. Junga, Dr. A. J. Matzger, Dr. F. Scherhag, M. Shim
Department of Chemistry, University of California at Berkeley
and
The Chemical Sciences Division, Lawrence Berkeley National Laboratory
Berkeley, CA 94720 (USA)
Fax: (+1) 510-643-5208
E-mail: vollhard@cchem.berkeley.edu

[**] This work was supported by the National Science Foundation (CHE-9610430). C.E. and F.S. thank the Deutsche Forschungsgemeinschaft for postdoctoral fellowships. A.J.M. was a Syntex predoctoral (1994 – 1995) and an ACS Division of Organic Chemistry Graduate Fellow (1995 – 1996), the latter sponsored by Rohm and Haas Co. We are indebted to Dr. K. Oertle (Ciba-Geigy AG) for a gift of chlorodimethyl(1,1,2-trimethylpropyl)silane and Professors J. M. Schulman and P. von R. Schleyer for preprints of their work.

  1433-7851/99/3806-0800 $ 17.50+.50/0

each benzene ring exhibits the same local symmetry and the molecules differ only in the sense of their overall connectivity.[1a, 6] Finally, they function as additional tests of the accuracy of contemporary calculational techniques, for which the phenylenes have proven to be attractive targets.[2, 3, 5, 6] We report herein the synthesis of the parent systems **1a** and **2a** and those of their respective derivatives **1b**, **2b**, and **2c**, the latter prepared in order to obtain X-ray structural details.

The initial strategy to the zigzag [4]phenylene frame **1** was patterned after that executed en route to its angular topomer,[1a] exploiting the regiocontrol exhibited by the Pd-catalyzed alkynylation of 1,2-diiodobiphenylene **3**, but inverting the sequence in which the two alkyne substituents are attached (Scheme 1).[7] The resulting compound **4** was then

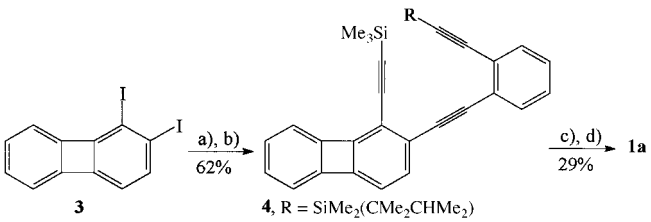

Scheme 1. a) *o*-$(HC_2)C_6H_4(C_2R)$ (1.2 equiv; R see Scheme), 10% CuI, 10% $[PdCl_2(PPh_3)_2]$, Et_3N, 23 °C, 15 h; b) Me_3SiC_2H (10 equiv), 7% CuI, 6% $[PdCl_2(PPh_3)_2]$, 50 °C, 2 d; c) $Bu_4N^+F^-$, THF, 23 °C, 40 min; d) $[CpCo(CO)_2]$ (0.9 equiv), *m*-xylene, △, *hν*, 18 h (syringe addition of **4**).

deprotected and cyclized in the presence of $[CpCo(CO)_2]$ to furnish **1a**. As the latter did not crystallize in a manner conducive to an X-ray investigation, an improved synthesis was developed which also provided crystalline **1b**. By starting with the selective, stepwise alkynylation of 1,2,3,4-tetrabromobenzene,[1c] the cumbersome construction of **3** was bypassed,[1a] and the basic carbon frame was assembled by a cobalt-catalyzed cyclization of pentayne **5** in one step to give **1b** (Scheme 2, Figure 1).[7, 8] The latter is novel, in as much as it constitutes the first such cooligomerization that is both intra- and intermolecular. Protodesilylation of **1b** resulted in **1a**.

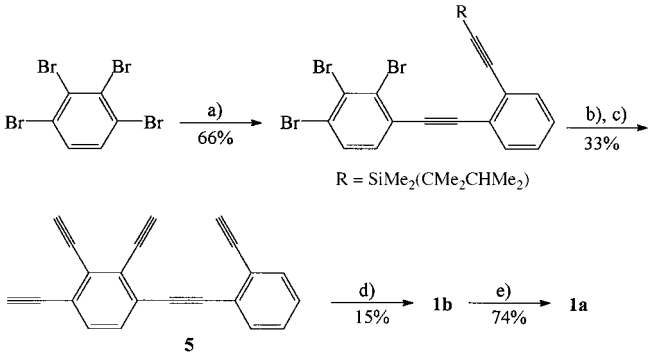

Scheme 2. a) *o*-$(HC_2)C_6H_4(C_2R)$ (0.2 equiv; R see Scheme), 6% CuI, 6% $[PdCl_2(PPh_3)_2]$, Et_3N, 50 °C, 24 h; b) Me_3SiC_2H (45 equiv), 30% CuI, 30% $[PdCl_2(PPh_3)_2]$, piperidine, 100 °C, 7 d; c) $Bu_4N^+F^-$, THF, 23 °C, 2 h; d) $(CH_3)SiC_2Si(CH_3)_3$ (solvent), $[CpCo(CO)_2]$ (2.0 equiv), △, *hν*, 10 h (syringe addition of **5**); e) $CF_3CO_2H/CHCl_3$ (1:25), 23 °C, 12 h.

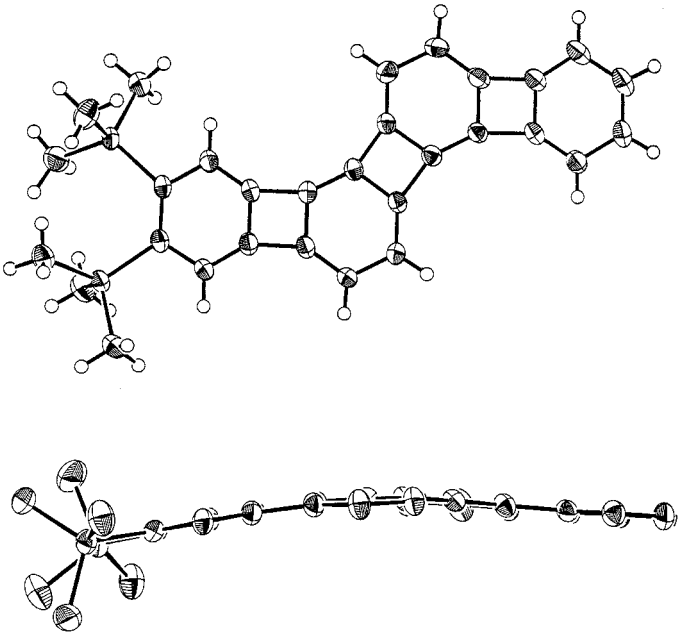

Figure 1. Structure of **1b** in the crystal: views from above (top) and the side (bottom).

Scheme 3 summarizes the construction of **2a**–**c**[7] through a variant of an improved route to the angular [5]phenylene nucleus,[1c] in which the hexaynes **6** are employed as substrates in the final cyclization. X-ray structures were obtainable on crystals of both **2b** and **2c** (Figure 2).[8]

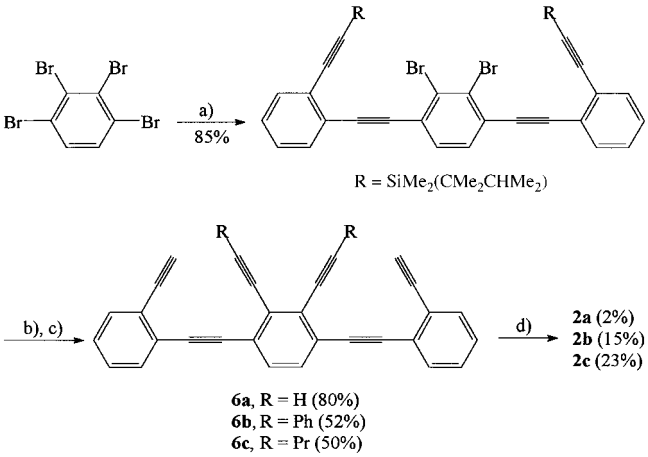

Scheme 3. a) *o*-$(HC_2)C_6H_4(C_2R)$, (R see Scheme), 3% CuI, 3% $[PdCl_2(PPh_3)_2]$, Et_3N, 23 °C, 5 d; b) RC_2H (20–100 equiv; R = $SiMe_3$, Ph, Pr), 1–2% CuI, 1–2% $[PdCl_2(PPh_3)_2]$, piperidine, 80 °C, 1–3 d; c) $Bu_4N^+F^-$, THF, 23 °C, 2 h; d) $[CpCo(CO)_2]$ (1 equiv), *m*-xylene, △, *hν*, 1–2 h (syringe addition of **6**).

Inspection of the spectral data of these systems (Table 1) is most instructive when the compounds are compared with each other and with the respective isomeric topologies. Thus, the electronic spectra bear the typical features of the phenylenes, with two sets of bands, one at higher energies exhibiting relatively large ε values, the other in the long wavelength range with much diminished intensity.[1a] As predicted by theory,[2b–d] the highest wavelength absorptions are much less bathochromically shifted (and hence the HOMO–LUMO

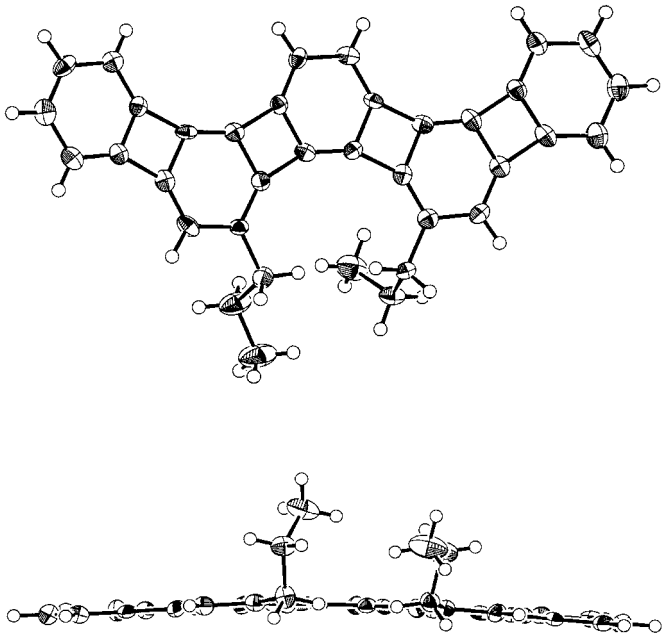

Figure 2. Structure of **2c** in the crystal: views from above (top) and the side (bottom).

gap less rapidly diminished) along the zigzag series ([3]- → [4]- →[5]phenylene; λ_{max} 428 →464 →484 nm) than those of its linear counterpart (λ_{max} 432 →492 →530 nm). Interestingly, however, **1a** and **2a** exhibit distinctive (albeit small, $\Delta\lambda_{max} \sim$ 15 nm) shifts of their highest wavelength bands to lower energy, relative to those of their respective angular relatives, indicative of an associated longitudinal transition dipole moment.[9] In contrast, the ^{1}H NMR spectra of the zigzag phenylenes are almost identical to those of their angular isomers, the "internal" benzene hydrogen atoms revealing incremental deshielding compared to the linear phenylenes and relative to angular [3]phenylene ($\delta = 6.18$). The corresponding shifts are: **1a**: $\delta_{Ha} = 6.27$, $\delta_{Hb} = 6.34$; **2a**: $\delta_{Ha} = 6.23$, $\delta_{Hb} = 6.26$, $\delta_{Hc} = 6.51$. This effect can be attributed to the cumulative influence of bond alternation in the internal benzene nuclei, resulting in relatively lesser paratropicity of the inside compared to the outside cyclobutadienoid rings, a view supported by nucleus-independent chemical shift (NICS) calculations.[6a] Theoretical estimates[5a, 6a,c,d,g] also predict zigzag fusion in the [N]phenylenes to be energetically advantaged over linear fusion (e.g. $\Delta\Delta H_f^\circ$ (linear →zigzag) ≈ $-(4.6-4.7)$ kcal mol^{-1} for $N = 4$, $\approx -(7.1-10.4)$ kcal mol^{-1} for $N = 5$) and, curiously, the zigzag topology to be slightly more stable ($\Delta\Delta H_f^\circ \approx 0.1-0.2$ kcal mol^{-1}) than the angular one (HF/6-31G* and B3LYP/6-31G*). The ^{13}C NMR data of the respective zigzag (e.g. **1a**, **2c**) and angular topomers[1a,c] are virtually superimposable ($\Delta\delta < 2$). In short, the spectral data indicate strong similarities between the zigzag and angular topological series (at least up to $N = 5$), both pronouncedly deviating in comparison to those of the linear phenylenes.

The X-ray data on **1b**, **2b**, and **2c** corroborate these observations structurally and demonstrate the effect of one- and twofold angular benzocyclobutadienannelation of angular [3]phenylene (Figure 3).

Table 1. Selected physical data for **1a**, **1b**, **2a – c**, and **8**.[7]

1a: light yellow powder, m.p. > 265 °C (decomp); MS (70 eV): *m*/*z* (%): 300 ([M^+], 100), 298 (25), 150 (10); ^{1}H NMR (400 MHz, $CDCl_3$): $\delta = 6.90-6.86$ (m, 4H), 6.82 – 6.77 (m, 4H), 6.34 (d, $J = 6.7$ Hz, 2H), 6.27 (d, $J = 6.7$ Hz, 2H); ^{13}C{^{1}H} NMR (100 MHz, $CDCl_3$): $\delta = 150.9$, 150.2, 149.5, 147.3, 137.2, 135.6, 128.8, 128.4, 119.0, 118.1, 116.5, 114.4; IR (KBr): $\tilde{\nu} = 3054$, 1448, 1414, 1360, 1345, 1252, 1156, 1057, 936, 834, 820, 746, 731 cm^{-1}; UV/Vis (THF): λ_{max} (lgε) = 256 (4.14), 278 (4.44), 284 (4.47), 299 (4.76), 313 (5.03), 338 (4.28), 356 (4.33), 376 (4.29), 399 (3.93), 465 (3.15) nm. High-resolution MS calcd for $C_{24}H_{12}$: 300.093900; found: 300.093896.

1b: light orange crystals, m.p. 209 – 210 °C; MS (70 eV): *m*/*z* (%): 444 ([M^+], 100), 429 (8), 413 (15), 371 (10), 356 (12), 341 (8), 207 (10), 168 (12), 73 (25); ^{1}H NMR (400 MHz, $CDCl_3$): $\delta = 7.12$ (s, 2H), 6.89 (m, 2H), 6.80 (m, 2H), 6.39 (d, $J = 6.7$ Hz, 1H), 6.34 (d, $J = 6.4$ Hz, 1H), 6.31 (d, $J = 6.8$ Hz, 1H), 6.28 (d, $J = 6.4$ Hz, 1H), 0.36 (s, 9H), 0.35 (s, 9H); ^{13}C{^{1}H} NMR (100 MHz, $CDCl_3$): $\delta = 151.3$, 150.8, 150.2, 149.8, 149.5, 148.6, 148.4, 147.9, 147.4, 147.2, 138.2, 137.1, 135.9, 135.7, 128.8, 128.3, 124.4, 123.6, 118.9, 118.1, 116.6, 116.4, 114.7, 114.4, 2.17, 2.15; IR (KBr): $\tilde{\nu} = 2953$, 1543, 1509, 1458, 1411, 1345, 1247, 1055, 855, 828, 754, 730, 669 cm^{-1}; UV/Vis (THF): λ_{max} (lgε) = 259 (4.22), 289 (4.51), 304 (4.77), 318 (4.99), 3.41 (4.30), 361 (4.34), 381 (4.31), 468 (3.06) nm. High-resolution MS calcd for $C_{30}H_{28}Si_2$: 444.172958; found: 444.172806.

2a: dark orange powder, M.p. > 260 °C (decomp); MS (70 eV): *m*/*z* (%): 374 ([M^+], 100), 372 (18), 187 (10), 78 (34), 69 (46), 57 (48), 55 (50); ^{1}H NMR (300 MHz, CD_2Cl_2): $\delta = 6.93-6.89$ (m, 4H), 6.86 – 6.79 (m, 4H), 6.51 (s, 2H), 6.26, 6.23 (AB, $J = 6.6$ Hz, 4H); UV/Vis (CH_2Cl_2): λ_{max} (lgε) = 315 (3.97), 326 (4.01), 350 (3.78), 366 (3.79), 484 (2.45) nm. High-resolution MS calcd for $C_{30}H_{14}$: 374.1096; found: 374.1098.

2b: orange-yellow crystals, M.p. > 300 °C; MS (70 eV): *m*/*z* (%): 526 ([M^+], 100), 446 (15), 263 (18), 149 (6); ^{1}H NMR (500 MHz, $CDCl_3$): $\delta = 7.31$ (dd, $J = 7.2$, 1.0 Hz, 4H), 6.98 – 6.93 (m, 4H), 6.89(m, 2H), 6.86(m, 2H), 6.78 (br dd, $J = 7.8$, 7.4 Hz, 4H), 6.68 (br dd, $J = 7.5$, 7.4 Hz, 2H), 6.58 (s, 2H), 6.42 (s, 2H); ^{13}C{^{1}H} NMR and DEPT 90 (100 MHz, $CDCl_3$): $\delta = 151.0$ (C), 150.2 (C), 148.9 (C), 147.7 (C), 143.3 (C), 138.5 (C), 136.1 (C), 135.5 (C), 134.6 (C), 131.2 (C), 128.8 (CH), 128.7 (CH), 128.6 (CH), 128.2 (CH), 125.9 (CH), 119.0 (CH), 118.4 (CH), 116.1 (CH), 115.5 (CH); IR (KBr): $\tilde{\nu} = 3053$, 1415, 1336, 1149, 814, 744, 737, 694 cm^{-1}; UV/Vis (CH_2Cl_2): λmax (lgε) = 261 (sh, 4.71), 280 (4.82), 321 (4.93), 339 (4.78), 362 (4.59), 382 (4.64), 446 (4.06), 476 (4.04), 504 (3.60) nm. High-resolution MS calcd for C_{42} H_{22}: 527.1755; found: 527.1758.

2c: yellow crystals, m.p. 269 – 270 °C; MS (70 eV): *m*/*z* (%): 458 ([M^+], 100), 413 (14), 398 (5), 229 (12), 207 (13), 199 (10), 91 (15), 57 (9); ^{1}H NMR (400 MHz, $CDCl_3$): $\delta = 6.96-6.91$ (m, 4H), 6.83 – 6.79 (m, 4H), 6.49 (s, 2H), 6.13 (s, 2H), 2.44 (t, $J = 7.5$, Hz, 4H), 1.63 (sex, $J = 7.5$ Hz, 4H), 0.97 (t, $J = 7.4$, Hz, 6H); ^{1}H NMR (500 MHz, CD_2Cl_2): $\delta = 6.96-6.91$ (m, 4H), 6.89 – 6.82 (m, 4H), 6.54 (s, 2H), 6.18 (s, 2H), 2.46 (t, $J = 7.3$ Hz, 4H), 1.63 (sex, $J = 7.3$ Hz, 4H), 0.99 (t, $J = 7.4$ Hz, 6H); ^{13}C{^{1}H} NMR (100 MHz, CD_2Cl_2): $\delta = 150.9$, 150.8, 149.6, 147.8, 145.0, 137.7, 135.3, 134.8, 132.4, 128.9, 128.8, 119.1, 118.5, 116.9, 116.4, 34.4, 23.4, 13.7; IR (KBr): $\tilde{\nu} = 3059$, 2953, 2928, 2869, 1415, 1340, 1158, 867, 829, 742 cm^{-1}; UV/Vis (CH_2Cl_2): λ_{max} (lgε) = 278 (4.37), 318 (4.81), 327 (4.83), 350 (sh, 4.57), 371 (4.65), 381 (sh, 4.61), 400 (sh, 4.30), 444 (3.90), 488 (3.48) nm. High-resolution MS calcd for $C_{36}H_{26}$: 458.2035; found: 458.2040.

8: pale yellow crystals, m.p. > 200 °C (decomp); MS (70 eV): *m*/*z* (%): 490 ([M^+], 100), 461 (9), 368 (12), 289 (10), 256 (18); ^{1}H NMR (400 MHz, CD_2Cl_2): $\delta = 7.50-7.38$ (m, 4H), 7.08 (d, $J = 7.3$ Hz, 1H), 7.00 (m, 2H), 6.98 (d, $J = 7.4$ Hz, 1H), 6.97 (m, 1H), 6.92 (m, 1H), 6.34 (t, $J = 1.6$ Hz, 1H), 6.17 (s, 1H), 2.34 – 2.14 (m, 4H), 1.68 – 1.42 (m, 4H), 1.01 (t, $J = 7.4$ Hz, 3H), 0.89 (t, $J = 7.3$ Hz, 3H); IR (KBr): $\tilde{\nu} =$ 3070, 2962, 2927, 2855, 1687, 1262, 1097, 1018, 802, 744 cm^{-1}.

Because the structural features of **2c** are identical within experimental error with those of its angular isomer,[1c] we can be confident that the following arguments apply equally to both the zigzag and angular series. Thus, in angular [3]phenylene, maximizing the aromatic π delocalization in the terminal benzene rings (in addition to σ strain effects)[1a] causes

  1433-7851/99/3806-0802 $ 17.50+.50/0 *Angew. Chem. Int. Ed.* **1999**, *38*, No. 6

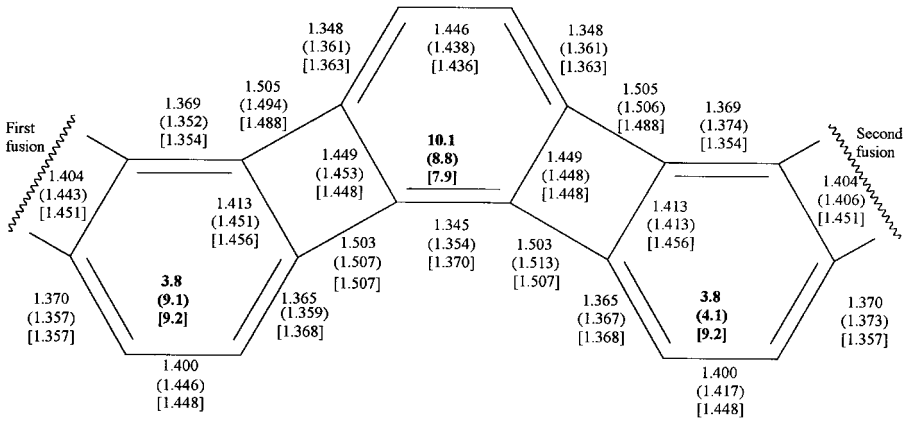

Figure 3. Comparative bond length data [Å] for angular [3]phenylene,[1a] the unsubstituted portion of **1b** (in parentheses), and the internal fragment of **2c** (in brackets; numbers are averaged for ideal symmetry). Bold numbers indicate the extent of bond alternation (in pm) according to the equation [Σ single bonds – Σ double bonds]/3 (× 100).

pronounced bond alternation in the central cyclohexatriene. Additional single annelation of one terminus, as in **1**, compromises delocalization in the latter, thus attenuating the extent of bond alternation of the "original" cyclohexatriene, that is in **1** the two internal benzenes are less π-bond localized than their counterpart in angular [3]phenylene, while the terminal six-membered rings (exemplified in Figure 3 for **1b** by its unsilylated end) remain essentially unchanged. A second annelation, as in **2**, has more subtle consequences, arguably (considering standard deviations and the presence of substituents in **2b** and **2c**) reinforcing bond alternation in the noncentral internal benzene rings, while somewhat attenuating it in the central ring. The terminal benzene nuclei (not shown in Figure 3) again retain a geometry essentially identical to that of their counterparts in angular [3]- and zigzag [4]phenylene, with minimal bond alternation and, as a consequence, considerably shortened bonds of fusion to the adjacent four-membered rings, signaling relatively stronger cyclobutadienoid, hence paratropic, character in the latter (compared to their "inside" counterparts), in agreement with NICS calculations[6a] and ^{1}H NMR data (vide supra). It is noteworthy that the experimental structural data are reproduced closely by calculations (for the parent systems)[5a, 6d,g] at the HF/6-31G*, and even better at the B3LYP/6-31G* density functional levels. Finally, the previously observed[1b,c] and calculated[2a, 5a, 6c,d,g] ready deformability of the phenylenes is evident in Figures 1 and 2 (side views). For **1b** the dihedral angles between the mean planes of adjacent rings range from 0.94 to 5.62°, for **2b** from 0.59 to 2.55°, and for **2c** from 1.15 to 2.53°.

While a thorough investigation of the chemistry for **1** and **2** will be the subject of future efforts, some preliminary experiments on **2c** appear to be consistent with the conclusions presented above. Thus, **2c** is inert to catalytic hydrogenation under conditions (5% Pd/C, 12.2 atm (180 psi)) which lead to hexahydro angular [3]phenylene,[1a] and, in contrast to angular [3]phenylene,[10] it does not react with dimethyl butynedioate in the presence of $AlCl_3$, indicative of lesser cyclohexatrienic reactivity.

Interestingly, however, the compound (in CH_2Cl_2) transforms (albeit in low yield), slowly in air, faster on exposure to O_2, while irradiating with visible light, to give enyne-(*Z*)-dione **8**,[7, 8] stereo- and regiospecifically, possibly through perepoxide **7** (Scheme 4), in analogy to the similar oxidation of linear [3]phenylene,[1a] perhaps signaling increased activation of the affected benzene nuclei relative to the central ring. The spectral data of **8** are as expected for a substituted angular [3]phenylene, and the X-ray determination reveals a highly nonplanar frame (Figure 4) with a distorted ten-membered ring in which the double bond, the two oxo functions, and the fused benzene rings are held at relatively large angles to each other.

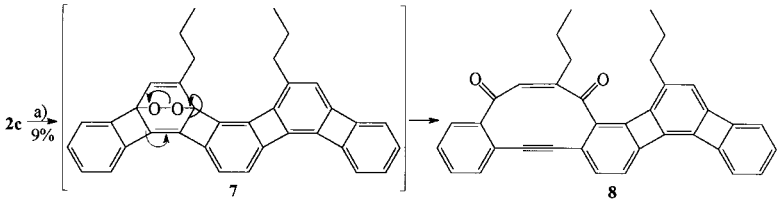

Scheme 4. a) O_2, *hν*, 12 h.

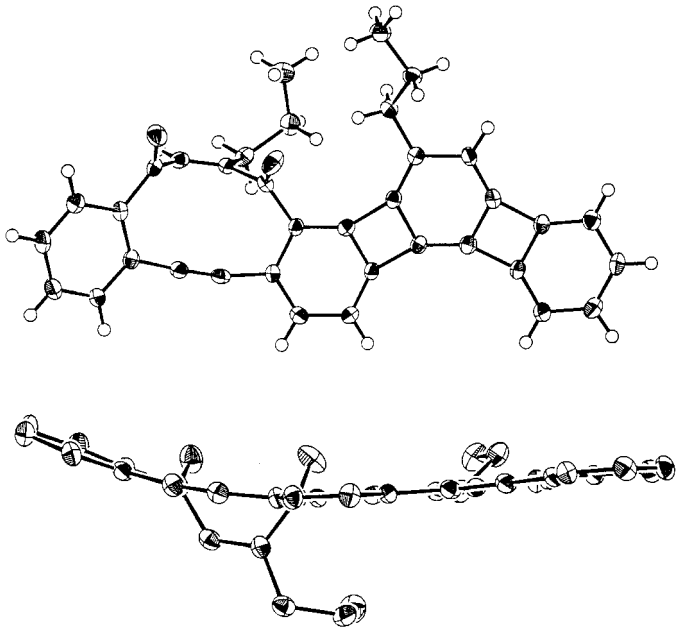

Figure 4. Structure of **8** in the crystal: views from above (top) and the side (bottom).

Received: October 9, 1998 [Z12511IE]
German version: *Angew. Chem.* **1999**, *111*, 856–860

Keywords: antiaromaticity · hydrocarbons · phenylenes · polycycles · strained molecules

  1433-7851/99/3806-0803 $ 17.50+.50/0

[1] a) D. L. Mohler, K. P. C. Vollhardt in *Advances in Strain in Organic Chemistry*, *Vol. 5* (Ed.: B. Halton), JAI, London, **1996**, pp. 121 – 160; b) R. Boese, A. J. Matzger, D. L. Mohler, K. P. C. Vollhardt, *Angew. Chem.* **1995**, *107*, 1630 – 1633; *Angew. Chem. Int. Ed. Engl.* **1995**, *34*, 1478 – 1481; c) C. Eickmeier, H. Junga, A. J. Matzger, F. Scherhag, M. Shim, K. P. C. Vollhardt, *Angew. Chem.* **1997**, *109*, 2194 – 2199; *Angew. Chem. Int. Ed. Engl.* **1997**, *36*, 2103 – 2108.

[2] a) A. Rajca, A. Safronov, S. Rajca, C. R. Ross II, J. J. Stezowski, *J. Am. Chem. Soc.* **1996**, *118*, 7272 – 7279; b) M. Baumgarten, F. Dietz, K. Müllen, S. Karabunarliev, N. Tyutyulkov, *Chem. Phys. Lett.* **1994**, *221*, 71 – 74; c) N. Trinajstic, T. G. Schmalz, T. P. Živković, S. Nikolić, G. E. Hite, D. J. Klein, W. A. Seitz, *New. J. Chem.* **1991**, *15*, 27 – 31; d) J. L. Brédas, R. H. Baughman, *J. Polym. Sci. Polym. Lett. Ed.* **1983**, *21*, 475 – 479.

[3] a) R. H. Baughman, D. S. Galvão, C. Cui, Y. Wang, D. Tománek, *Chem. Phys. Lett.* **1993**, *204*, 8 – 14; b) R. H. Baughman, H. Eckhardt, M. Kertesz, *J. Chem. Phys.* **1987**, *87*, 6687 – 6699; c) A. T. Balaban, C. C. Rentia, E. Ciupitu, *Rev. Roum. Chim.* **1968**, *13*, 231 – 247.

[4] a) B. I. Dunlap, R. Taylor, *J. Phys. Chem.* **1994**, *98*, 11018 – 11019; b) M. M. Mestechkin, G. T. Klimko, G. E. Vaiman, V. A. Panichkina, *Zh. Strukt. Khim.* **1992**, *33*, 8 – 14.

[5] a) J. M. Schulman, R. L. Disch, *J. Am. Chem. Soc.* **1996**, *118*, 8470 – 8474; b) J. M. Schulman, R. L. Disch, *Chem. Phys. Lett.* **1996**, 262, 813 – 816; c) A. D. Haymet, *Chem. Phys.* Lett. **1985**, *122*, 421 – 424.

[6] a) J. M. Schulman, R. L. Disch, H. Jiao, P. von R. Schleyer, *J. Phys. Chem. A* **1998**, *102*, 8051 – 8057; b) I. Gutman, S. Klavžar, *ACH-Models Chem.* **1998**, *135*, 45 – 55, and references therein; c) J. M. Schulman, R. L. Disch, *J. Phys. Chem. A* **1997**, *101*, 5596 – 5599; d) Z. B. Maksić, D. Kovaček, M. Eckert-Maksić, M. Böckmann, M. Klessinger, *J. Phys. Chem.* **1995**, *99*, 6410 – 6416; e) I. Gutman, *S. Afr. J. Chem.* **1994**, *47*, 53 – 55; f) I. Gutman, *J. Chem. Soc. Farad. Trans.* **1993**, *89*, 2413 – 2416; g) A. J. Matzger, K. P. C. Vollhardt, unpublished results.

[7] All new isolated compounds gave satisfactory analytical and/or spectral data (see Table 1).

[8] X-ray structural analyses: **1b**: Crystal size $0.38 \times 0.34 \times 0.20\ mm^3$, space group $P2_1/c$ (no. 14), scan range $3 < 2\theta < 52.30^\circ$, $a = 16.5909(3)$, $b = 9.1224(1)$, $c = 17.5914(2)$ Å, $\beta = 108.089(1)^\circ$, $V = 2430.84(8)$ Å^3, $Z = 4$, $\rho_{calcd} = 1.167\ g\,cm^{-3}$, $\mu = 1.55\ cm^{-1}$, 4743 unique reflections at $-85\,^\circ C$, of which 3320 were taken as observed $[F_o > 3.00\sigma(F)]$, $R = 0.036$, $R_w = 0.046$. **2b:** Crystal size $0.30 \times 0.25 \times 0.20\ mm^3$, space group *Pbcn* (no. 60), scan range $4.00 > 2\theta > 45.00$, $a = 22.9475(3)$, $b = 12.8479(2)$, $c = 8.7785(2)$ Å, $V = 2588.14(7)$ Å^3, $Z = 4$, $\rho_{calcd} = 1.351\ g\,cm^{-3}$, $\mu = 0.77\ cm^{-1}$, 2582 unique reflections at $-101\,^\circ C$, of which 1551 were taken as observed $[F_o > 3.00\sigma(F)]$, $R = 0.037$, $R_w = 0.042$. **2c**: Crystal size $0.25 \times 0.10 \times 0.10\ mm^3$, space group $P2_12_12_1$ (no. 19), scan range $4.00 < 2\theta < 45.00^\circ$, $a = 25.3045(3)$, $b = 5.3273(1)$, $c = 18.5416(4)$ Å, $V = 2499.49(7)$ Å^3, $Z = 4$, $\rho_{calcd} = 1.219\ g\,cm^{-3}$, $\mu = 0.69\ cm^{-1}$, 4270 unique reflections at $-108\,^\circ C$, of which 2444 were taken as observed $[F_o > 3.00\sigma(F)]$, $R = 0.054$, $R_w = 0.065$. **8**: Crystal size $0.41 \times 0.24 \times 0.02\ mm^3$, space group *Pbca* (no. 61), scan range $3.00 < 2\theta < 45.00^\circ$, $a = 20.9160(5)$, $b = 7.5075(2)$, $c = 32.6655(7)$ Å, $V = 5129.35(29)$ Å^3, $Z = 8$, $\rho_{calcd} = 1.270\ g\,cm^{-3}$, $\mu = 0.77\ cm^{-1}$, 4210 unique reflections at $-118\,^\circ C$, of which 1873 were taken as observed $[F_o > 3.00\sigma(F)]$, $R = 0.029$, $R_w = 0.030$. Crystallographic data (excluding structure factors) for the structures reported in this paper have been deposited with the Cambridge Crystallographic Data Center as supplementary publication no. CCDC-103129 (**8**), 103130 (**2c**), 103131 (**2b**), 103132 (**1b**). Copies of the data can be obtained free of charge on application to CCDC, 12 Union Road, Cambridge CB2 1EZ, UK (fax: (+44) 1223-336-033; e-mail: deposit@ccdc.cam.ac.uk).

[9] a) H. H. Jaffé, M. Orchin, *Theory and Applications of Ultraviolet Spectroscopy*, Wiley, New York, **1962**, chap. 13; b) for electronic excitation spectra of biphenylene, see: M. E. Beck, R. Rebentisch, G. Hohlneicher, M. P. Fülscher, L. Serrano-Andrés, B. O. Roos, *J. Chem. Phys.* **1997**, *107*, 9464 – 9474, and references therein; c) for a similar observation in dibenzobiphenylenes, see: M. P. Cava, J. F. Stucker, *J. Am. Chem. Soc.* **1955**, *77*, 6022 – 6026; J. W. Barton, *J. Chem. Soc.* **1964**, 5161 – 5164.

[10] S. Kumaraswamy, A. J. Matzger, K. P. C. Vollhardt, unpublished results.

Coordinative Approach to Mediated Electron Transfer: Ruthenium Complexed to Native Glucose Oxidase**

Ekaterina S. Ryabova, Vasily N. Goral, Elisabeth Csöregi, Bo Mattiasson, and Alexander D. Ryabov*

Mediated electron transfer to or from active sites of oxidoreductases[1] is often accomplished by covalent binding of a redox-active species either to the enzyme surface[2–5] or to the enzyme active site.[6] Transition metal complexes such as ferrocene derivatives and osmium compounds are most commonly used. In addition, there are reports on using ruthenium compounds;[7, 8] however, these did not find widespread application, and this seems rather surprising taking into account the lower cost of Ru compounds and their higher reactivity toward glucose oxidase (GO)[9] with respect to related Os complexes. Also, an attractive feature of ruthenium complexes of the type *cis*-$[Ru(LL)_2Cl_2]$ (LL = bpy or phen-type ligands) is associated with their ability to coordinate monodentate nitrogen donor ligands like pyridine or imidazole (Q) [Eq. (1)].

$$cis\text{-}[Ru(LL)_2Cl_2] + Q \rightleftharpoons cis\text{-}[Ru(LL)_2ClQ]^+Cl^- \quad (1)$$

If proteins are considered as potential ligands, enzymes appear to be superior, since many of them, including oxidoreductases, contain histidine residues in their active sites. Therefore, it was anticipated that the interaction between an enzyme and *cis*-$[Ru(LL)_2Cl_2]$ would result in binding of the ruthenium center to the imidazole side chain of histidine in such a way that it is delivered close to the active site and thus provides an efficient electron transfer relay (Scheme 1). Glucose oxidase from *A. niger* is a very advantageous enzyme because it contains two imidazole side chains, His 516 and H 559, close to FAD.[10] Therefore we decided to carry out a "coordinative" loading of the complexes *cis*-$[Ru(LL)_2Cl_2]$ (LL = bpy (**1**) and phen (**2**)) into GO and to investigate electrocatalytic characteristics of ruthenium-modified GO (Ru(LL)-GO). As a result, we succeeded in

[*] Prof. A. D. Ryabov
Department of Chemistry, Moscow State University
119899, Moscow (Russia)
and
G. V. Plekhanov Russian Economic Academy
Stremyanny per. 28, 113054, Moscow (Russia)
Fax: (+7) 095-939-5417
E-mail: ryabov@enzyme.chem.msu.su

E. S. Ryabova, V. N. Goral
Department of Chemistry, Moscow State University
119899, Moscow (Russia)

Dr. E. Csöregi, Prof. B. Mattiasson
Department of Biotechnology, Center for Chemistry and Chemical Engineering
Lund University
P.O. Box 124, S-221 00 Lund (Sweden)

[**] Financial support from the Russian Foundation for Basic Research (Grant No 96-03-34328a), INTAS (Project 1432), and a fellowship from the Swedish Institute for ESR is gratefully acknowledged. We thank Den Bokhan for experimental assistance. Abbreviations: FAD: flavin adenine dinucleotide; GO: glucose oxidase.

  1433-7851/99/3806-0804 $ 17.50+.50/0